

Article

Retention of Hydraulic Fracturing Water in Shale: The Influence of Anionic Surfactant

Hesham Abdulelah ^{1,*}, Syed M. Mahmood ^{1,*}, Sameer Al-Hajri ²,
Mohammad Hail Hakimi ³ and Eswaran Padmanabhan ¹

¹ Shale Gas Research Group (SGRG), Institute of Hydrocarbon Recovery, Faculty of Petroleum & Geoscience, Universiti Teknologi PETRONAS, Seri Iskandar 32610, Perak, Malaysia;

eswaran_padmanabhan@utp.edu.my

² Department of Petroleum Engineering, Universiti Teknologi PETRONAS, Seri Iskandar 32610, Perak, Malaysia; ensamyo87@gmail.com

³ Geology Department, Faculty of Applied Science, Taiz University, 6803 Taiz, Yemen; ibnalhakimi@yahoo.com

* Correspondence: heshamsaif09@gmail.com (H.A.); mohammad.mahmood@utp.edu.my (S.M.M.); Tel.: +60-1139628761 (H.A.); +60-5368-7103 (S.M.M.)

Received: 16 October 2018; Accepted: 26 November 2018; Published: 30 November 2018



Abstract: A tremendous amount of water-based fracturing fluid with ancillary chemicals is injected into the shale reservoirs for hydraulic fracturing, nearly half of which is retained within the shale matrix. The fate of the retained fracturing fluid is raising some environmental and technical concerns. Mitigating these issues requires a knowledge of all the factors possibly contributing to the retention process. Many previous studies have discussed the role of shale properties such as mineralogy and capillarity on fracturing fluid retention. However, the role of some surface active agents like surfactants that are added in the hydraulic fracturing mixture in this issue needs to be understood. In this study, the influence of Internal Olefin Sulfate (IOS), which is an anionic surfactant often added in the fracturing fluid cocktail on this problem was investigated. The effect on water retention of treating two shales “BG-2 and KH-2” with IOS was experimentally examined. These shales were characterized for their mineralogy, total organic carbon (TOC) and surface functional groups. The volume of retained water due to IOS treatment increases by 131% in KH-2 and 87% in BG-2 shale. The difference in the volume of retained uptakes in both shales correlates with the difference in their TOC and mineralogy. It was also inferred that the IOS treatment of these shales reduces methane (CH₄) adsorption by 50% in KH-2 and 30% in BG-2. These findings show that the presence of IOS in the composition of fracturing fluid could intensify water retention in shale.

Keywords: hydraulic fracturing; water retention in shale; anionic surfactant; shale gas

1. Introduction

Shale gas reservoirs are known to have ultra-porosity and permeability, thus exploiting them through conventional production methods is not economically feasible [1,2]. Hydraulic fracturing combined with horizontal drilling has been implemented to enhance gas production from shale, and they were proven to be commercial and effective approaches [3–5]. The aim of hydraulic fracturing in shale is to promote its permeability by opening the existing natural fractures and generating new fractures. It is accomplished by injecting a large volume of water-based fluid down a well at a suitable rate and pressure. The resulting fracture networks within shale are typically kept open with proppants to encourage the gas flow from shale to the producing well thus improving gas recovery [6,7]. The fracking fluid is generally composed of water (~99.5%), proppants and a mixture of chemical additives that vary depending on the characteristics of shale reservoir [8,9].

One of the significant issues associated with fracking in shale is that massive amount of fracturing fluid (~5–50%) is retained in the formation after the fracking process [10,11]. For example, Ge [9] and Penny et al. [12] reported that only around 5% of the water is recovered the fracturing processes in shale while Nicot et al. [13] found less than 20%. Yang et al. [4], Makhnov et al. [14] and Reagan et al. [15] disclosed lower than 30% of fracking fluid in some other shale plays to flow-back whereas the other 70% of the injected fluid is believed to be retained by the shale reservoir. In some areas of the Barnett and Marcellus shales, the recovered water after fracking was nearly 50% [9,16].

The fracking water retention issue in shale has raised environmental [17–20] and technical concerns [21,22]. The role of retained water in contaminating the drinking water aquifers is a topic of debate [17]. Vidic et al. [20] stated that the induced fractures outside the target formation could provide pathways for fracking fluid to migrate through. In the town of Pavillion, WY, the U.S. Environmental Protection Agency (EPA) observed water contamination in two shallow monitoring wells [18]. Elevated levels of pH, specific conductance and traces of gas were confirmed in shallow groundwater possibly due to retained fracking water [23]. In Garfield County, the salinity of groundwater was reported to increase with fracking activities in the nearby wells [24]. The rise in salinity with increasing the number of oil and gas wells could trigger the claim that migration from oil/gas wells nearby took place thus contaminating the shallow groundwater [17]. Similarly, an official report by EPA [19] proposed that local water well in West Virginia was found contaminated with gel; conceivably due to leakage of fracturing fluid from an adjacent vertically fractured well. Birdsell et al. [25] concluded based on a two-dimensional conceptual model that the risk of aquifer contamination is reduced ten times by the combined influence of production well and capillary imbibition. Myers [26] estimated the risk of groundwater contamination by fracking water by applying groundwater transport model to a Marcellus shale utilizing the pressure data from a gas well. He found that fracking fluid might reach groundwater aquifers in less than ten years. In Europe, investigating the possible in-situ contamination risk of hydraulic fracturing operation has gained considerable attention. The European Union (EU) has recently sponsored a project called “FracRisk” to explore the likely risks of the fracking operation. Under the “FracRisk” project, some generic and modeling studies were carried out to assess the potential impact of hydraulic fracturing on groundwater aquifers [27,28]. The amount of water used for hydraulic fracturing in shale is massive, the considerable proportion of retained fracturing fluid will necessitate using even more water which will adversely affect the water resources in some shale gas areas, which endure water scarcity [29]. Besides its possible environmental issues, the retained fracking water can significantly impair the production of shale gas. Ge et al. [19], Gallegos et al. [29] and Sharma et al. [30] explained that retention of fracturing fluid was found to develop the water saturation near surfaces of the created fractures, which can prominently impact the gas relative permeability and productivity. Gas production will be significantly reduced as the water saturation reaches 40–50% [31,32].

Mitigating the issue of fracturing fluid retention in shale requires knowledge about the factors controlling this phenomenon. In the literature, more focus was given to the role of shale mineralogy [33] as a significant factor governing water retention during hydraulic fracturing. Many of the published studies [21,34,35] reports that clays, which are one of the primary minerals in shale have the affinity to imbibe water molecules due to their hydrophilic nature. However, the effect of some surface acting agents’ that are added into the fracking fluid mixture on water retention in shale was not given enough focus. Common chemical additives in fracturing fluid are often surfactants [7,34,36–38]. Generally, they are intended to increase the viscosity of fracturing fluid to allow it to propagate within the target formation. An anionic surfactant that is added in fracturing fluid mixture is Internal Olefin Sulfate (IOS) [34].

Shales have a mixed-charged surface due to the coexistence of negative surface-charged and positive surface-charged minerals. Anionic surfactants have a negatively charged headgroup and positively charged weak tail. Figure 1 presents a depiction of the interaction between an anionic surfactant and a shale surface. Once anionic surfactant solution comes into contact with shale surface,

either its strong headgroup will be attracted to the positively charged site (Figure 1a), or its weak tail will be attracted to the negatively charged sites in shale (Figure 1b). These interactions between the anionic surfactant and shale can alter its wettability and thus causing its water imbibition behavior to increase or decrease [34,39].

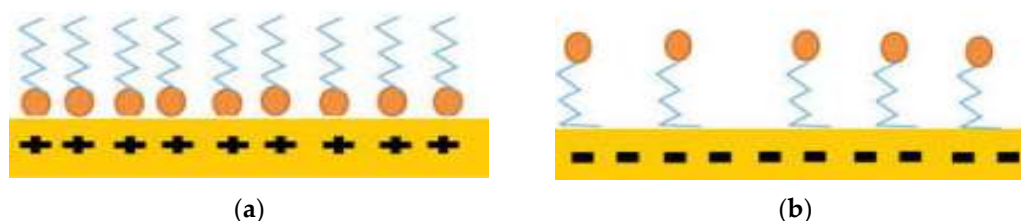


Figure 1. Schematic diagram of the electrostatic interaction between (a) surfactant headgroup and positive-charged sites in shale, and (b) surfactant weak tail and negative-charged sites in shale. Modified after Zhou et al. [39].

In this study, the effect of IOS (anionic surfactant) on water retention in two Malaysian shales was investigated. The shales were characterized for their total organic carbon (TOC), mineralogy, topology, and pore system. Water retention was then examined in two ways; measurements of water uptakes [40] and by utilizing the U.S Bureau of Mine Method (USBM) [34] adsorption/desorption method.

2. Materials and Methods

2.1. Shales

Table 1 lists the properties of the shales used in this study. The two shales differ in their mineralogy and the amount of organic carbon. The two shale shales were collected from two different Paleozoic black shale formations in Peninsular Malaysia. One shale “BG-2” was taken from Batu Gajah formation in Perak district. Batu Gajah formation was described by Baioumy et al. [41] to be a Carboniferous black shale outcrop formation composed of grey and black flaggy shales. The other shale “KH-2” was obtained from Kroh formation in Kedah district, which comes under the Ordovician-Devonian age. The Kroh formation is composed of a sequence of black carbonaceous shale and mudstone.

Table 1. Properties of the BG-2 and KH-2 shales.

Sample ID	Color	Geological Age	Thermal Maturity	Formation	Country
BG-2	Grey	Carboniferous *	Over-matured *	Batu Gajah	Malaysia
KH-2	Black	Ordovician-Devonian *	Over-matured *	Kroh	Malaysia

* Baioumy et al. [41].

2.2. Surfactant

IOS was used to treat the two shales in this study. Table 2 shows the available information about this surfactant. Surfactants are added into the hydraulic fracturing fluid to control its viscosity. In Bakken shale, a surfactant formulation including IOS was used to understand its imbibition behavior [42]. IOS is also suitable to be used in hydraulic fracturing processes [43].

Table 2. Properties of IOS obtained from supplier and literature.

Commercial Name	Type	Key Properties	Supplier
ENORDET O332	Anionic surfactant	Appearance: Colorless. Liquid at room temperature; pH: 9–12 Density: 0.7 g/cm ³ density at 23 °C Active matter (%): 28.03 Carbon atoms numbers: 15–18 Critical micelle concentration: 0.05% *	SHELL

* Abdulelah et al. [34].

The chemical structure of IOS is shown in Figure 2. It has two alkyl groups (R) with 15 to 18 carbon atoms on the tail [44]. To achieve the highest change in wettability, IOS was used at a concentration of 1 wt.%, which is well above its critical micelle concentration (CMC).

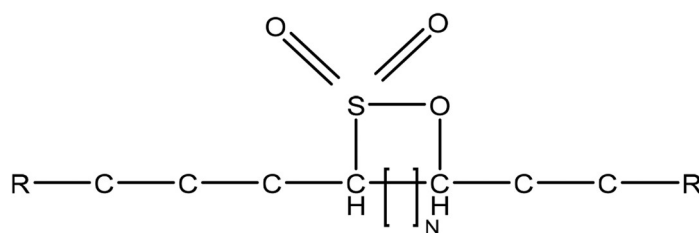


Figure 2. Chemical structure of Internal Olefin Sulfate (IOS).

2.3. Mineralogy and Topology

The mineralogy of the two shales was studied using x-ray diffractometer (Model: XPert3, PANalytical, Seri Iskandar, Malaysia). Powder forms of BG-2 and KH-2 shales were scanned from 5° to 65° with a step size of 0.026° . The basic principle of this technique is that electrons are produced from an X-ray tube and then accelerated towards the sample (shale in this study). Typical x-ray spectra are generated once electrons collide with the sample. The sample is continuously rotated by a motor, and the intensity of diffracted X-rays at an angle (2θ) is plotted. The interatomic spacing (d) is computed using Bragg's law. Each D spacing value is a signature of some minerals that are then identified by comparing these values with the database.

The elements that constitute the mineralogy of both shales were investigated utilizing energy dispersive spectrometry (EDS) by a microscope (ZEISS, Seri Iskandar, Malaysia) at an accelerating voltage of 20 kV. Visualization of the mineralogy and pores in BG-2 and KH-2 shales was acquired exploiting Field Emission Scanning Electron Microscopy (FE-SEM, Model: Zeiss Supra 55VP). The fundamental of EDS and Images is that electrons beam is focused onto the sample surface hence producing secondary electrons, backscattered electrons, and characteristics X-ray. Both secondary and backscattered electrons are used for imaging. Characteristics X-ray is used for EDS. FE-SEM follow the same working principle but produces higher resolution images than SEM [45].

2.4. TOC

Total carbon (TC) analyzer (Model: Multi N/C 3100, Analytik Jena, Seri Iskandar, Malaysia) was utilized to measure the percentage of the TOC in BG-2 and KH-2 shales. Before the measurements, the two shales were treated with Hydrochloric acid (HCL) of 37% concentration to remove the inorganic carbon. The TC analyzer utilizes the combustion approach to determine the TOC. After the sample is loaded into a ceramic boat, the amount of carbon is then determined by combustion in an oxygen environment at 1200°C . The resulted carbon dioxide is then measured by a detector, and then carbon % can be calculated.

2.5. Fourier-Transform Infrared Spectroscopy (FTIR)

The FTIR spectra of the two shales "BG-2 and KH-2" were obtained using a Perkin Elmer (Seri Iskandar, Malaysia) spectrometer. The measurements were carried out to obtain the abundant structures in both shales. The procedures for FTIR spectroscopy involve emitting a photon to a molecule hence exciting it to higher energy level. The molecular bonds at the higher energy state vibrate at varying wavenumber. Each wavenumber corresponds to a particular functional group (e.g., C=O) [46]. FTIR spectroscopy has been utilized by many researchers to decipher the existing functional groups in many materials including but not limited to rocks [46,47] and chemicals [48]. In this study, FTIR was carried out to unravel the surface functional groups in the two shales to support the mineralogy and TOC results. Before the measurements, the two shales were dried for 12 h.

2.6. Wettability Measurement

To assess the affinity of the two shales towards water and surfactant solution, contact angles between the polished shale surfaces and water/surfactant solution were measured. The measurements were obtained using Vinci's interfacial tension meter (IFT, model IFT 700, Vinci Technology, Seri Iskandar, Malaysia) by the Sessile Drop Method. The baseline wettability of the two shales was assessed using a droplet of pure water on their polished surfaces. Their wettability for anionic surfactants was then determined using a droplet of 1 wt.% IOS solution.

2.7. Direct Measurement of Water Retention

The water retention phenomenon in the two shales was evaluated utilizing the conventional natural stone method [49] at ambient condition under two cases; baseline and with IOS solution. The procedure includes immersing 100 g of each shale in pure water/surfactant solution in a desiccator under continuous vacuuming to remove the trapped air noted. When equilibrium was achieved, the retained water for the two shales was then calculated using mass balance.

2.8. Indirect Measurement of Water Retention

Figure 3 displays the schematic of the adsorption column used in this study. It is well known from the literature that water retention in shale impairs gas flow [19,30,31,50]. The measurements were carried out to investigate the change in gas adsorption in "BG-2 and KH-2" shales due to treatment by IOS solution. To achieve that, the pressure across the adsorption column was monitored during CH₄ adsorption.

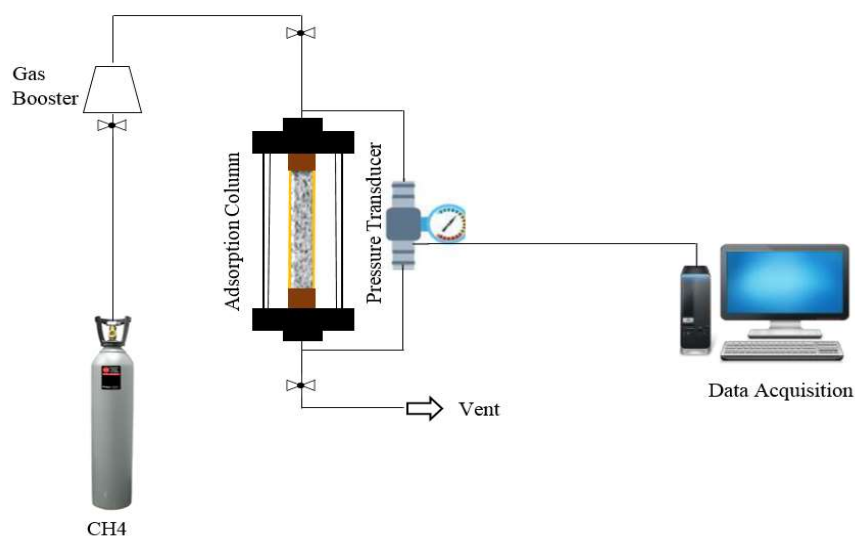


Figure 3. Schematic of Adsorption/Desorption Experimental Set-up.

The readings were then plotted versus time to unravel the adsorption behavior under the effect of water retention. The investigation was carried out in "BG-2 and KH-2" shales before and after treatment with 1wt.% of IOS solution. The U.S Bureau of Mines (USBM) adsorption procedures were followed [34].

3. Results and Discussion

3.1. Mineralogy of Shales

The mineralogy results from X-ray Powder Diffraction (XRD) of the two shales "BG-2 and KH-2" used in this study are presented in Table 3. It can be seen that BG-2 shale contains a higher amount of

clay and a lower amount of non-clay minerals as compared to KH-2. The difference in mineralogy in both shales will help better explain the water retention results.

Table 3. Quantitative mineralogy of BG-2 and KH-2 shales from XRD measurement.

Sample ID	Non-Clay Minerals (wt.%)				Clay Minerals (wt.%)							
	Quartz	Kpsar	Clacite	Total (%)	Kaolinite	Smectite	Illite	Chlorite	Muscovite	Biotite	Dickite	Total (%)
BG-2	29.3	12.8	1.3	43.4	6.3	12.7	23.1	5	9.3	0.1	NA	56.6
KH-2	66	7.2	0.8	74.5	2.8	9.7	9.7	1.9	NA	0.9	0.5	25.5

The FE-SEM images of the two shales are shown in Figure 4. The platy/flaky structure of grains indicates the presence of clay. It can be seen that BG-2 (a) shale has more clay as compared to the KH-2 shale (b), which supports the XRD results.

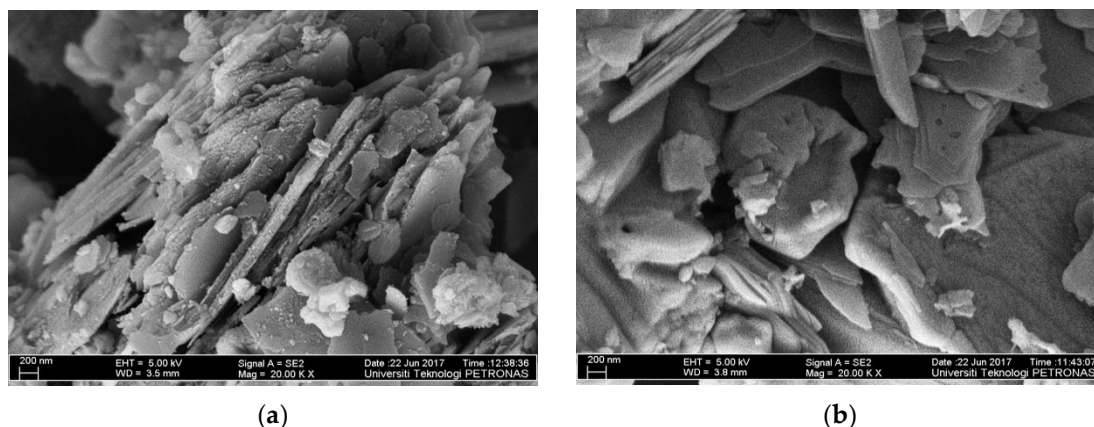


Figure 4. FE-SEM images for (a) BG-2 and (b) KH-2 shales.

The Energy-Dispersive X-Ray (EDX) spectra for BG-2 (a) and KH-2 (b) shales is shown in Figure 5 with a corresponding miniature image of Figure 4 embedded in the graph for ease of comparison.

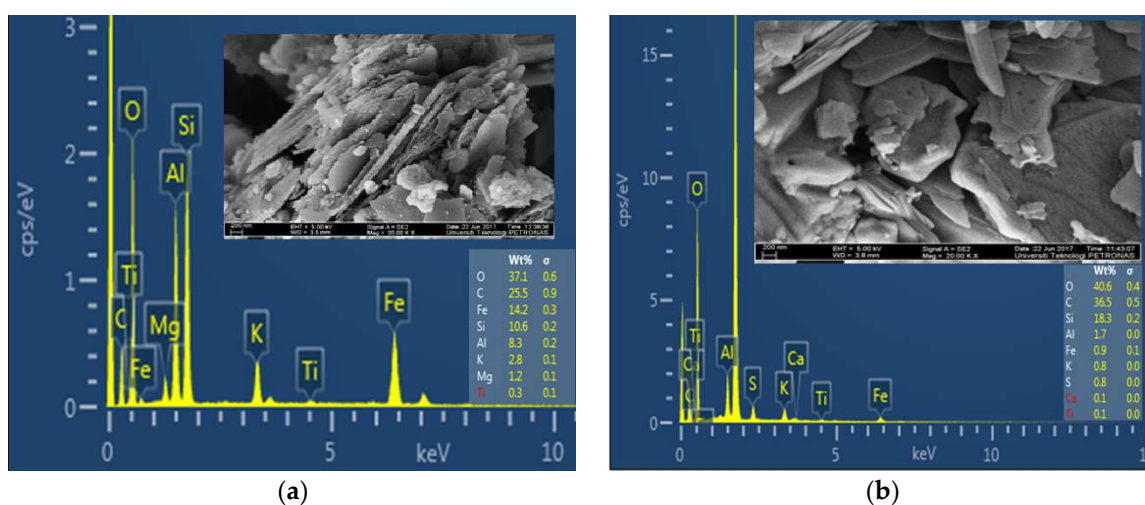


Figure 5. The Energy-Dispersive X-Ray (EDX) spectra of (a) BG-2 and (b) KH-2 shales with a corresponding miniature FE-SEM images.

The BG-2 shale spectrum shows high values of counts per second per electron-volt (cps/eV) at around 1.5 and 1.7 KeV identify Al and Si minerals respectively, thus indicating the presence of iron-rich platy crystals of clays such as kaolinite (Si, Al) and/or illite (Al, Si, K, Fe). While comparing the elements of KH-2 with BG-2, it is found that KH-2 shale is richer in carbon (C) and silicon (Si). However, it is lower in aluminum (Al), potassium (K), and iron (Fe). Furthermore, it contains a trace of calcium as opposed to magnesium (Mg) that was found in BG-2. Thus, the KH-2 shale is richer in silica and organic matters and has a lower clay content.

3.2. TOC

Figure 6 shows that KH-2 has a TOC of 12.1%, while BG-2 has only 2.1%. TOC is associated with the presence of organic matter in the shale. From the perspective of wettability, the organic matter contributes towards the hydrophobicity of shale [34]. As such, KH-2 is presumably more hydrophobic than BG-2.

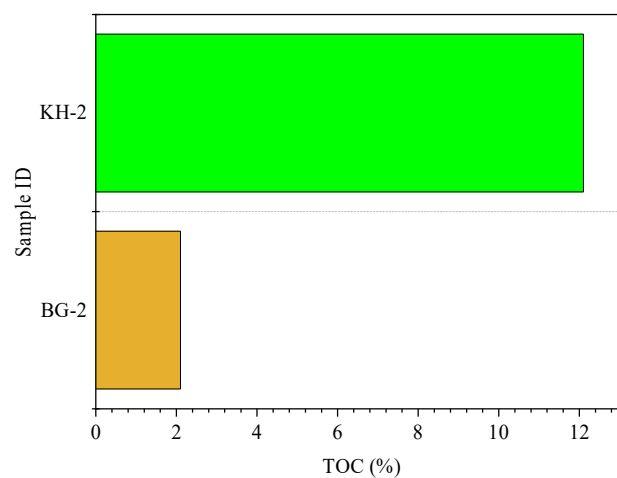


Figure 6. The total organic carbon (TOC) percentage in BG-2 and KH-2 shales.

3.3. Fourier-Transform Infrared Spectroscopy (FTIR)

Figure 7 presents the FTIR spectra of BG-2 and KH-2 shales. The broadband existing between 3404 and 3627 cm^{-1} probably corresponds to O-H stretching of hydroxyl groups which could be attributed to the existence of clay minerals.

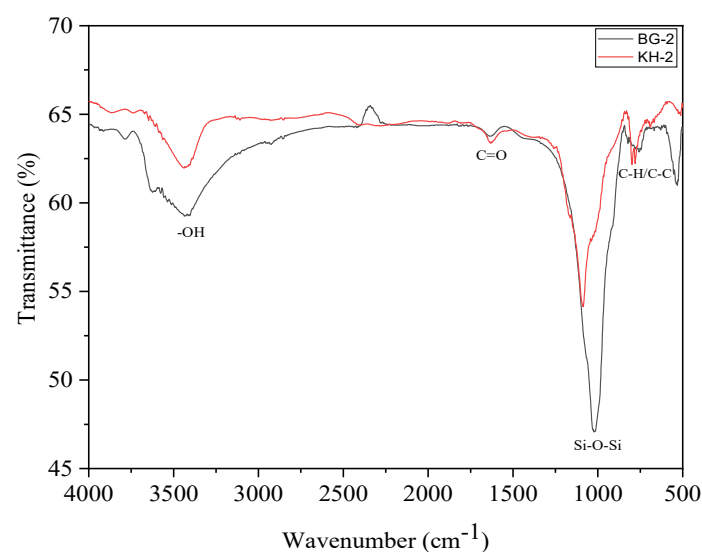


Figure 7. Fourier-Transform Infrared Spectroscopy (FTIR) Spectrum of BG-2 and KH-2 shales.

The presence of clay minerals and quartz is also inferred from the stretching of Si–O–Si band at about 1021 cm^{-1} [51]. The intensity of these bands in BG-2 is greater than KH-2 inferring that BG-2 is richer in clay than KH-2, which confirms XRD results in Table 3. The presence of organic matter is evidenced by the peaks at 1635 cm^{-1} and 676 cm^{-1} . These peaks are attributed to C=O vibration of carboxylates and deformation of CH group; respectively. These two functional groups come from organic matter [51–53].

3.4. Wettability

Figure 8 display the wettability results by contact angle method of BG-2 (a) and KH-2 (b) shales with pure water and IOS solution. The presented contact angles are the average of the contact angles taken throughout three minutes to ensure the stability of the recorded contact angles. The lower contact angle of a solution on a surface indicates that it is more wetting than pure water. In BG-2 shale, the contact angle recorded with IOS solution was nearly 3.5° , which is lower than the contact angle with pure water that was about 22° . Therefore, it can be deduced that IOS solution was more wetting than pure water for BG-2 shale. Similar but less obvious behavior was seen in KH-2 shale, where a contact angle of approximately 19.5° was measured with IOS solution compared to 37° contact angle obtained with pure water.

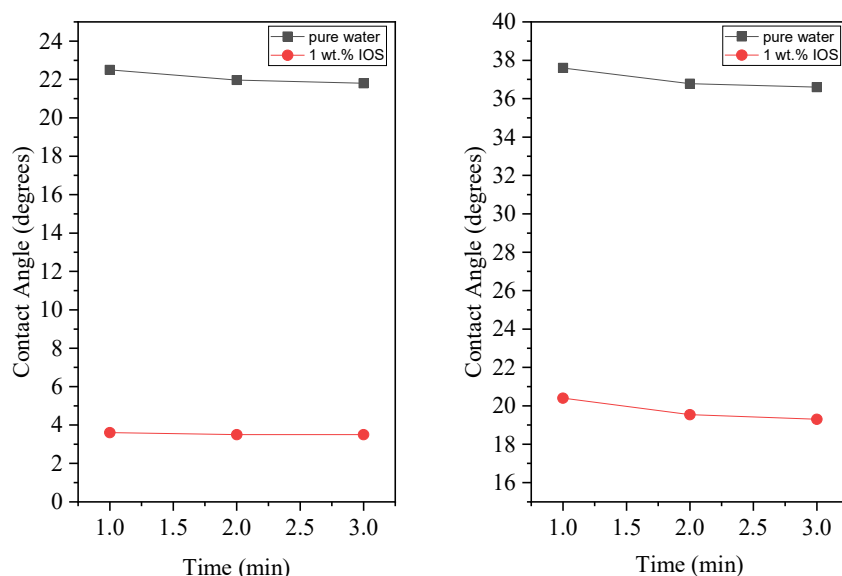


Figure 8. Measured contact angles at (a) BG-2 shale surface with pure water and 1 wt.% IOS solution (b) KH-2 shale surface with pure water and 1wt.% IOS solution.

3.5. Water Uptake

Figure 9 displays the water uptake volume in BG-2 and KH-2 shales before and after treatment with 1 wt.% of IOS solution. The amount of retained water in both shales increased significantly after treating the shales with the IOS solution. When BG-2 shale was immersed in pure distilled water, the volume of water uptake was noted to be 11.2 mL. It increased to 21 mL (an 87% increase) when immersed in a 1 wt.% IOS solution. Similar but less significant behavior was seen in KH-2 shale in which the amount of water uptake increased drastically from 8 mL in pure distilled water to 18.5 mL (a 131% increase) in 1 wt.% IOS solution. It is noteworthy to mention that the upsurge in water uptakes is possibly due to wettability alteration of shales by IOS towards more water wet. In a previous study [34] in two shales from the same formations, it was noticed that IOS changed the wettability of shales into more water- wet. These findings correlate well with the wettability results in Figure 8. IOS was more wetting than pure water in both shales hence imbining more than pure water.

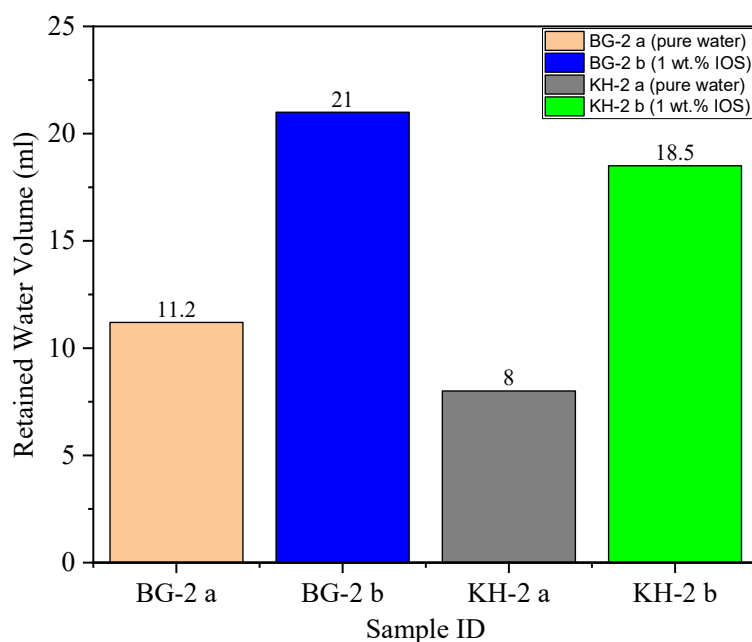


Figure 9. Water uptakes volume in BG-2 and KH-2 shales.

3.6. End Cycle Pressure vs. Time

The USBM's gas adsorption method was adopted in this study to study the adsorption behavior of shales. According to previous studies, water retention in shale was found to impair gas flow in shale. The decline in the quantity of adsorbed CH_4 was used to explain the water retention behaviors in both shales. More pressure drop during CH_4 adsorption process presumably indicates higher gas adsorption and vice versa. CH_4 adsorption in the two shales "BG-2 and KH-2" was performed before and after treatment with IOS surfactant and the pressure drop versus time was utilized to explain the water uptakes in both shales.

A crushed shale specimen (100 g) was placed in the adsorption column which was then closed/sealed and tested for gas leakage. The column was pressurized to 20 bar with CH_4 , and then the connection to the gas source was closed to isolate the chamber. The pressure was noted at the end of the 2 h adsorption cycle, and the valve connecting to the CH_4 source was re-opened momentarily, and the column was re-pressurized to 20 bar again. Ten of such cycles were repeated for each shale.

Figure 10 displays the pressure reading at the end of each cycle vs. time for BG-2 and KH-2 shales. The black curve is for pure distilled water treated while the red curve is for the IOS treated shale. In the case of pure distilled water treated shale, the pressure continued decreasing till the end of the 5th adsorption cycles (10 h) indicating the continued CH_4 adsorption. The pressure at the end of the 6th cycle was similar to the 5th cycle suggesting that the rate of adsorption is leveling off. The lowest pressure observed during the test was 14 bar (a 30% change in pressure), and it occurred after about 12 h. The pressure change at the end of each subsequent cycle became gradually smaller until the last two cycles in which there was no change in pressure indicating that CH_4 adsorption is completed. When BG-2 shale was treated with IOS, the end of cycle pressure profile drastically changed. The lowest pressure observed during the test was 18 bar (only 10% change in pressure), and it occurred after just the 1st cycle (2 h). The next two cycles saw a slow reduction of the end of cycle pressure, but there was no change in pressure reduction after the 5th cycle. When comparing the behavior of the two curves, it becomes evident that IOS treatment has reduced the adsorption capacity of the shale. For the pure distilled water treated KH-2 shale, the cycle end pressure continued decreasing till the end of the 4th adsorption cycles indicating the continued CH_4 adsorption. The pressures at the end of the 5th–7th cycles were similar to the 4th cycle suggesting that the rate of adsorption was leveling off.

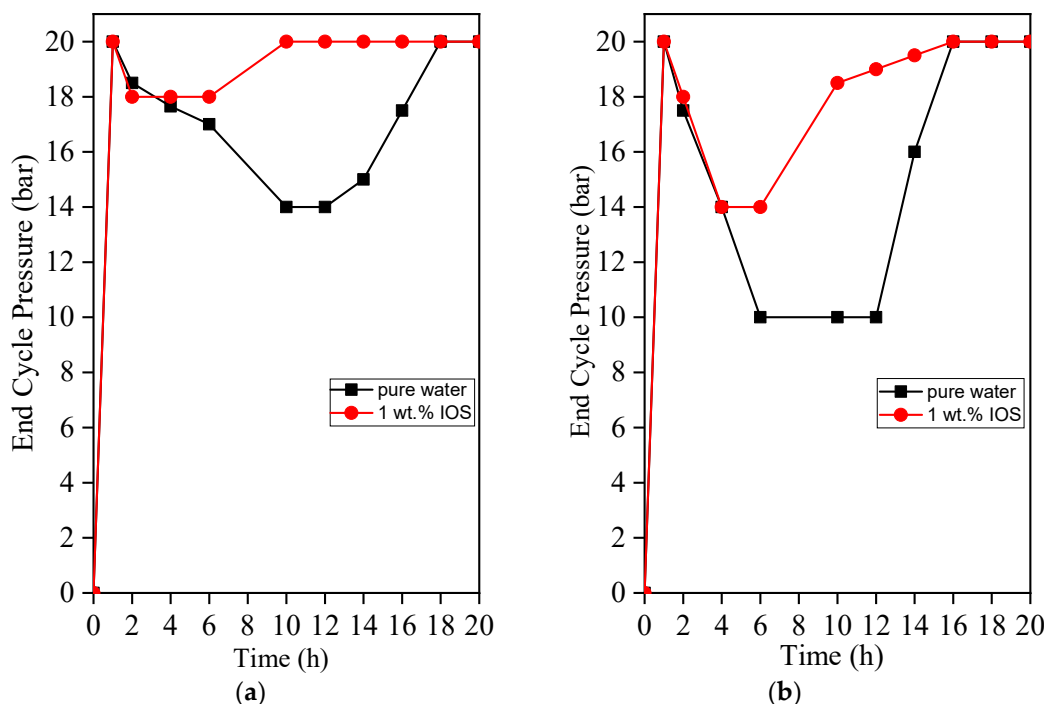


Figure 10. Column pressure at the end of adsorption cycle vs. time for (a) BG-2 and (b) KH-2 shales.

The lowest pressure observed during the test was 10 bar (a 50% change in pressure), and it occurred after about 6 h (3rd cycle). The pressure changes at the end of each subsequent cycle became gradually smaller until the last three cycles in which there was no change in pressure indicating that complete CH_4 adsorption was achieved. In the case of KH-2 that was treated with IOS, the end of cycle pressure profile significantly changed. The lowest pressure observed during the test was 14 bar (a 30% change in pressure), and it occurred after only the third cycle. The pressures at the end of 4th cycles were similar to the 3rd cycle suggesting no change in the rate of adsorption. The next four cycles saw a gradual reduction of the end of cycle pressure, but there was no change in pressure reduction after the 7th cycle. While comparing the behavior of the two curves, it becomes evident that IOS treatment has reduced the adsorption capacity of KH-2 shale.

Figure 11 shows a comparison of the two shales “BG-2 and KH-2” after treatment with pure distilled water only. The pressure at the end of each adsorption cycle was plotted vs. time. The solid curve is for KH-2 water-treated shale, while the dotted curve is for BG-2 water-treated shale. In the first adsorption cycle, a similar cycle-end pressure was noted in both shales. Later, KH-2 shale showed a more drastic change in cycle-end pressure till the end of the 3rd cycle (a 50% reduction in pressure). A less pronounced decrease in pressure was seen in BG-2 shale, where only a 30% reduction in pressure was noted at the end of the 5th cycle. When comparing the cycle-end pressure of the two shales, it becomes clear that the amount adsorbed CH_4 was more in KH-2 shale. It is most likely attributed to the fact that KH-2 is richer than BG-2 in organic matter.

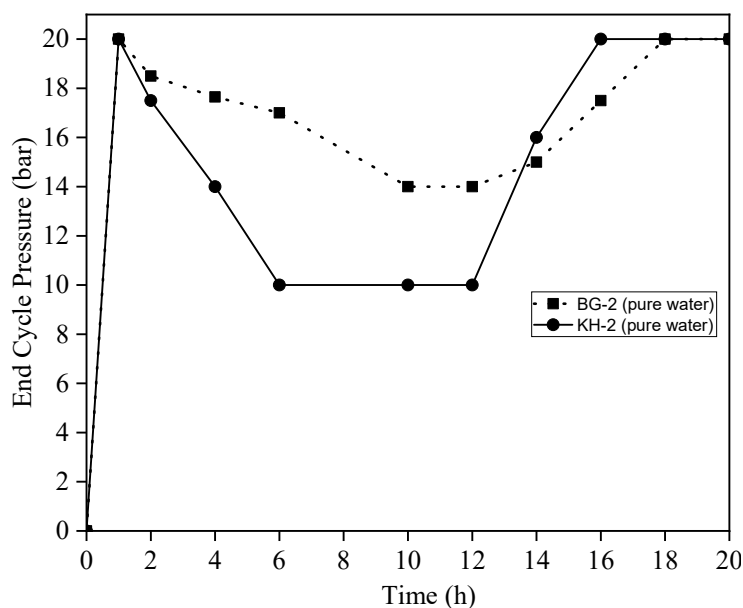


Figure 11. The end cycle adsorption pressure for BG-2 and KH-2 shales treated with pure water.

The adsorption behavior of the two shales “BG-2 and KH-2” after treatment with IOS is shown in Figure 12, where the end-cycle pressure is plotted vs. time. A reduction in pressure was noted in KH-2 shale (solid curve) up to the end of the 3rd cycle (a 30% reduction in pressure). However, it was not as significant as with the purely distilled water case cycle (was a 50% reduction in pressure). Less significant reduction in end-cycle pressure was seen in BG-2 shale, where only a 10% reduction in pressure was noted at the end of the 2nd cycle. When comparing the end cycle pressure reading in both shales, it is found that KH-2 showed higher CH₄ adsorption than BG-2, as was the case with pure water treatment.

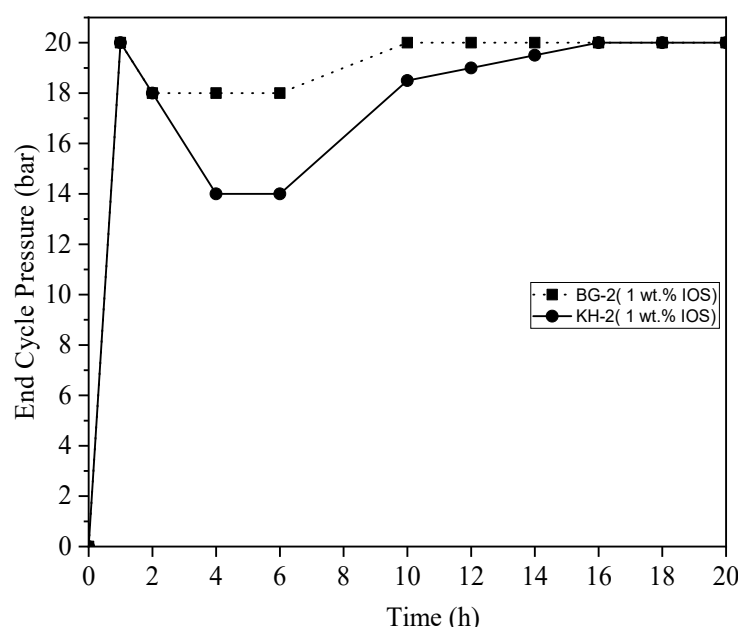


Figure 12. The end cycle adsorption pressure for BG-2 and KH-2 shales treated with IOS

It is evident from Figures 11 and 12 that IOS treatment has reduced the CH₄ adsorption in both shales as compared to pure water treatment. It should be noted that the IOS had increased the water retention in both shales as compared to pure water treatment. Presumably, the higher water retention in both shales occupied some of the available adsorption sites, thus resulting in lower gas adsorption.

4. Conclusions

In this study, the influence of anionic surfactant on water retention in shales was investigated. Two well-characterized Malaysian shales “BG-2 and KH-2” were treated with 1 wt.% IOS solution, and the changes in water uptake were noted. The water retention phenomenon was inferred from the results of the water imbibition and gas adsorption tests. When BG-2 and KH-2 shales were treated with 1 wt.% IOS solution, their water retention and CH₄ adsorption characteristics changed compared to the case when they were immersed in pure water. The water uptakes dramatically increased by 131% in KH-2 and 87% in BG-2, while CH₄ adsorption was reduced by 50% in KH-2 and 30% in BG-2. It is presumed that the higher water retention in both shales occupied some of the available adsorption sites, thus resulting in lower gas adsorption. The mineralogical analysis of the two shales showed that higher water retention and consequent lower gas adsorption was observed in BG-2 shale which had a higher clay content of 57% and low TOC of 2.1% as compared to the KH-2. The difference in the amount of retained water in both shales was found to correlate with their TOC and mineralogy. The higher affinity of BG-2 to retain a significant amount of water is possibly attributed to its high clay content and poor organic material. The relatively lower water uptake in KH-2 is presumably attributed to its high TOC of 12.1% and low clay content of 26%. As opposed to clay, organic matter is hydrophobic and thus hindering water imbibition. These results also suggest that the addition of anionic surfactant into the fracking fluid cocktail for hydraulic fracturing of shales could increase the water retention issue.

Author Contributions: Conceptualization, H.A.; methodology, H.A. and S.M.M.; software, S.A.-H.; validation, H.A., S.M.M. and M.H.H.; formal analysis, H.A.; investigation, H.A.; resources, S.M.M.; data curation, H.A. and M.H.H.; writing—original draft preparation, H.A.; writing—review and editing, S.A.-H., S.M.M. and H.A.; visualization, H.A. and S.M.M.; supervision, S.M.M. project administration, E.P.; funding acquisition, E.P.

Funding: This research was funded by Shale Gas Research Group (SGRG) and PRF-Research Grant (Cost Center 0153AB-A33).

Acknowledgments: We acknowledge the Shale Gas Research Group (SGRG) in UTP and Shale PRF project (cost center # 0153AB-A33) for the financial support. We also thank SHELL for providing the surfactant.

Conflicts of Interest: The authors declare no conflict of interest.

References

1. Mokhatab, S.; Poe, W.A. *Handbook of Natural Gas Transmission and Processing*; Gulf Professional Publishing: Boston, MA, USA, 2012.
2. Speight, J.G. *The Chemistry and Technology of Petroleum*; CRC Press: Boca Raton, FL, USA, 2014.
3. Novlesky, A.; Kumar, A.; Merkle, S. Shale Gas Modeling Workflow: From Microseismic to Simulation—A Horn River Case Study. In Proceedings of the 2011 Canadian Unconventional Resources Conference, Calgary, AB, Canada, 15–17 November 2011; p. 24.
4. Yang, L.; Ge, H.; Shi, X.; Cheng, Y.; Zhang, K.; Chen, H.; Shen, Y.; Zhang, J.; Qu, X. The effect of microstructure and rock mineralogy on water imbibition characteristics in tight reservoirs. *J. Nat. Gas Sci. Eng.* **2016**, *34*, 1461–1471. [CrossRef]
5. Rivard, C.; Lavoie, D.; Lefebvre, R.; Séjourné, S.; Lamontagne, C.; Duchesne, M. An overview of Canadian shale gas production and environmental concerns. *Int. J. Coal Geol.* **2014**, *126*, 64–76. [CrossRef]
6. Sydansk, R.D. Hydraulic Fracturing Process. U.S. Patent 5,711,376, 27 January 1998.
7. Atherton, F.; Bradfield, M.; Christmas, K.; Dalton, S.; Dusseault, M.; Gagnon, G.; Hayes, B.; MacIntosh, C.; Mauro, I.; Ritcey, R.; et al. Report of the Nova Scotia Independent Panel on Hydraulic Fracturing. Available online: <https://energy.novascotia.ca/sites/default/files/Report%20of%20the%20Nova%20Scotia%20Independent%20Panel%20on%20Hydraulic%20Fracturing.pdf> (accessed on 30 November 2018).
8. Cherry, J.; Ben-Eli, M.; Bharadwaj, L.; Chalaturnyk, R.; Dusseault, M.B.; Goldstein, B.; Lacoursière, J.-P.; Matthews, R.; Mayer, B.; Molson, J. *Environmental Impacts of Shale Gas Extraction in Canada*; Council of Canadian Academies: Ottawa, ON, Canada, 2014.

9. King, G.E. Hydraulic fracturing 101: What every representative, environmentalist, regulator, reporter, investor, university researcher, neighbor, and engineer should know about hydraulic fracturing risk. *J. Petrol. Technol.* **2012**, *64*, 34–42. [CrossRef]
10. Shen, Y.; Ge, H.; Meng, M.; Jiang, Z.; Yang, X. Effect of water imbibition on shale permeability and its influence on gas production. *Energy Fuels* **2017**, *31*, 4973–4980. [CrossRef]
11. Engelder, T.; Cathles, L.M.; Bryndzia, L.T. The fate of residual treatment water in gas shale. *J. Unconv. Oil Gas Resour.* **2014**, *7*, 33–48. [CrossRef]
12. Penny, G.S.; Dobkins, T.A.; Pursley, J.T. Field Study of Completion Fluids To Enhance Gas Production in the Barnett Shale. In Proceedings of the 2006 SPE Gas Technology Symposium, Calgary, AB, Canada, 15–18 May 2006; p. 10.
13. Nicot, J.-P.; Scanlon, B.R. Water use for shale-gas production in Texas, US. *Environ. Sci. Technol.* **2012**, *46*, 3580–3586. [CrossRef] [PubMed]
14. Makhonov, K.; Habibi, A.; Dehghanpour, H.; Kuru, E. Liquid uptake of gas shales: A workflow to estimate water loss during shut-in periods after fracturing operations. *J. Unconv. Oil Gas Resour.* **2014**, *7*, 22–32. [CrossRef]
15. Reagan, M.T.; Moridis, G.J.; Keen, N.D.; Johnson, J.N. Numerical simulation of the environmental impact of hydraulic fracturing of tight/shale gas reservoirs on near-surface groundwater: Background, base cases, shallow reservoirs, short-term gas, and water transport. *Water Resour. Res.* **2015**, *51*, 2543–2573. [CrossRef] [PubMed]
16. Sun, Y.; Bai, B.; Wei, M. Microfracture and surfactant impact on linear cocurrent brine imbibition in gas-saturated shale. *Energy Fuels* **2015**, *29*, 1438–1446. [CrossRef]
17. Vengosh, A.; Jackson, R.B.; Warner, N.; Darrah, T.H.; Kondash, A. A critical review of the risks to water resources from unconventional shale gas development and hydraulic fracturing in the United States. *Environ. Sci. Technol.* **2014**, *48*, 8334–8348. [CrossRef] [PubMed]
18. DiGiulio, D.C.; Wilkin, R.T.; Miller, C.; Oberley, G. Investigation of Ground Water Contamination Near Pavillion. Presented at the Wyoming Workgroup Meeting, Pavillion, WY, USA, 30 November 2011.
19. Ge, H.-K.; Yang, L.; Shen, Y.-H.; Ren, K.; Meng, F.-B.; Ji, W.-M.; Wu, S. Experimental investigation of shale imbibition capacity and the factors influencing loss of hydraulic fracturing fluids. *Pet. Sci.* **2015**, *12*, 636–650. [CrossRef]
20. Vidic, R.D.; Brantley, S.L.; Vandenbossche, J.M.; Yoxtheimer, D.; Abad, J.D. Impact of shale gas development on regional water quality. *Science* **2013**, *340*, 1235009. [CrossRef] [PubMed]
21. Cheng, Y. Impact of water dynamics in fractures on the performance of hydraulically fractured wells in gas-shale reservoirs. *J. Can. Pet. Technol.* **2012**, *51*, 143–151. [CrossRef]
22. Yan, Q.; Lemanski, C.; Karpyn, Z.T.; Ayala, L. Experimental investigation of shale gas production impairment due to fracturing fluid migration during shut-in time. *J. Nat. Gas Sci. Eng.* **2015**, *24*, 99–105. [CrossRef]
23. Wright, P.R.; McMahon, P.B.; Mueller, D.K.; Clark, M.L. *Groundwater-Quality and Quality-Control Data for Two Monitoring wells Near Pavillion, Wyoming, April and May 2012*; 2327-638X; US Geological Survey: Reston, VA, USA, 2012.
24. Thyne, G. Review of Phase II Hydrogeologic Study. Available online: [https://www.garfield-county.com/oil-gas/documents/Thyne%20FINAL%20Report%2012\[1\].20.08.pdf](https://www.garfield-county.com/oil-gas/documents/Thyne%20FINAL%20Report%2012[1].20.08.pdf) (accessed on 30 November 2018).
25. Birdsell, D.T.; Rajaram, H.; Dempsey, D.; Viswanathan, H.S. Hydraulic fracturing fluid migration in the subsurface: A review and expanded modeling results. *Water Resour. Res.* **2015**, *51*, 7159–7188. [CrossRef]
26. Myers, T. Potential contaminant pathways from hydraulically fractured shale to aquifers. *Groundwater* **2012**, *50*, 872–882. [CrossRef] [PubMed]
27. Taherdangkoo, R.; Tatomir, A.; Taylor, R.; Sauter, M. Numerical investigations of upward migration of fracking fluid along a fault zone during and after stimulation. *Energy Procedia* **2017**, *125*, 126–135. [CrossRef]
28. Tatomir, A.; McDermott, C.; Bensabat, J.; Class, H.; Edlmann, K.; Taherdangkoo, R.; Sauter, M. Conceptual model development using a generic Features, Events, and Processes (FEP) database for assessing the potential impact of hydraulic fracturing on groundwater aquifers. *Adv. Geosci.* **2018**, *45*, 185–192. [CrossRef]
29. Gallegos, T.J.; Varela, B.A.; Haines, S.S.; Engle, M.A. Hydraulic fracturing water use variability in the United States and potential environmental implications. *Water Resour. Res.* **2015**, *51*, 5839–5845. [CrossRef] [PubMed]

30. Sharma, M.; Agrawal, S. Impact of Liquid Loading in Hydraulic Fractures on Well Productivity. In Proceedings of the 2013 SPE Hydraulic Fracturing Technology Conference, The Woodlands, TX, USA, 4–6 February 2013; p. 16.
31. Shanley, K.W.; Cluff, R.M.; Robinson, J.W. Factors controlling prolific gas production from low-permeability sandstone reservoirs: Implications for resource assessment, prospect development, and risk analysis. *AAPG Bull.* **2004**, *88*, 1083–1121. [[CrossRef](#)]
32. Hematpour, H.; Mahmood, S.M.; Nasr, N.H.; Elraies, K.A. Foam flow in porous media: Concepts, models and challenges. *J. Nat. Gas Sci. Eng.* **2018**. [[CrossRef](#)]
33. Dehghanpour, H.; Lan, Q.; Saeed, Y.; Fei, H.; Qi, Z. Spontaneous imbibition of brine and oil in gas shales: Effect of water adsorption and resulting microfractures. *Energy Fuels* **2013**, *27*, 3039–3049. [[CrossRef](#)]
34. Abdulelah, H.; Mahmood, S.M.; Al-Mutarreb, A. The Effect of Anionic Surfactant on the Wettability of Shale and its Implication on Gas Adsorption/Desorption Behavior. *Energy Fuels* **2018**. [[CrossRef](#)]
35. Settari, A.; Sullivan, R.B.; Bachman, R.C. The Modeling of the Effect of Water Blockage and Geomechanics in Waterfracs. In Proceedings of the 2002 SPE Annual Technical Conference and Exhibition, San Antonio, TX, USA, 29 September–2 October 2002; p. 7.
36. Fisher, M.K.; Warpinski, N.R. Hydraulic-fracture-height growth: Real data. *SPE. Prod. Oper.* **2012**, *27*, 8–19. [[CrossRef](#)]
37. Huynh, U.T. *Surfactant Characterization to Improve Water Recovery in Shale Gas Reservoirs*; The University of Texas at Austin: Austin, TX, USA, 2013.
38. Patel, P.S.; Robart, C.J.; Ruegamer, M.; Yang, A. Analysis of US Hydraulic Fracturing Fluid System and Proppant Trends. In Proceedings of the 2014 SPE Hydraulic Fracturing Technology Conference, The Woodlands, TX, USA, 4–6 February 2014; p. 20.
39. Zhou, L.; Das, S.; Ellis, B.R. Effect of surfactant adsorption on the wettability alteration of gas-bearing shales. *Environ. Eng. Sci.* **2016**, *33*, 766–777. [[CrossRef](#)]
40. Al-Mutarreb, A.; Jufar, S.R.; Abdulelah, H.; Padmanabhan, E. Influence of Water Immersion on Pore System and Methane Desorption of Shales: A Case Study of Batu Gajah and Kroh Shale Formations in Malaysia. *Energies* **2018**, *11*, 1511. [[CrossRef](#)]
41. Baioumy, H.; Ulfa, Y.; Nawawi, M.; Padmanabhan, E.; Anuar, M.N.A. Mineralogy and geochemistry of Palaeozoic black shales from Peninsular Malaysia: Implications for their origin and maturation. *Int. J. Coal Geol.* **2016**, *165*, 90–105. [[CrossRef](#)]
42. Wang, D.; Butler, R.; Zhang, J.; Seright, R. Wettability survey in Bakken shale with surfactant-formulation imbibition. *SPE Reservoir Eval. Eng.* **2012**, *15*, 695–705. [[CrossRef](#)]
43. Semple, T.C.; Reznik, C.; Barnes, J.R.; Buechele, J.L.; Dubey, S.T.; King, T.E. Use of Long Chain Internal Olefin Sulfonates. U.S. Patent 2014/0353250 A1, 4 December 2014.
44. Nasr, N.H.; Mahmood, S.M.; Hematpur, H. A rigorous approach to analyze bulk and coreflood foam screening tests. *J. Pet. Explor. Prod. Technol.* **2018**, 1–14.
45. Mutalib, M.A.; Rahman, M.; Othman, M.; Ismail, A.; Jaafar, J. Scanning Electron Microscopy (SEM) and Energy-Dispersive X-Ray (EDX) Spectroscopy. In *Membrane Characterization*; Elsevier: Amsterdam, The Netherlands, 2017; pp. 161–179.
46. Chen, Y.; Zou, C.; Mastalerz, M.; Hu, S.; Gasaway, C.; Tao, X. Applications of micro-fourier transform infrared spectroscopy (FTIR) in the geological sciences—A review. *Int. J. Mol. Sci.* **2015**, *16*, 30223–30250. [[CrossRef](#)] [[PubMed](#)]
47. Cronauer, D.; Snyder, R.; Painter, P. Characterization of Oil Shale by FTIR Spectroscopy. Available online: https://web.anl.gov/PCS/acsfuel/preprint%20archive/Files/27_2_LAS%20VEGAS_03-82_0122.pdf (accessed on 28 November 2018).
48. Akbari, S.; Mahmood, S.M.; Tan, I.M.; Ghaedi, H.; Ling, O.L. Assessment of Polyacrylamide Based Co-Polymers Enhanced by Functional Group Modifications with Regards to Salinity and Hardness. *Polymers* **2017**, *9*, 647. [[CrossRef](#)]
49. En, U. *Natural Stone Test Methods-Determination of Water Absorption at Atmospheric Pressure*; British Standards Institution: London, UK, 2008.
50. Ford, W.G.; Penny, G.S.; Briscoe, J.E. Enhanced water recovery improves stimulation results. *SPE Prod. Eng.* **1988**, *3*, 515–521. [[CrossRef](#)]

51. Khraisheh, M.A.; Al-degs, Y.S.; McMinn, W.A. Remediation of wastewater containing heavy metals using raw and modified diatomite. *Chem. Eng. J.* **2004**, *99*, 177–184. [[CrossRef](#)]
52. Van der Marel, H.W.; Beutelspacher, H. *Atlas of Infrared Spectroscopy of Clay Minerals and Their Admixtures*; Elsevier Publishing Company: Amsterdam, The Netherlands, 1976.
53. Haberhauer, G.; Rafferty, B.; Strebl, F.; Gerzabek, M. Comparison of the composition of forest soil litter derived from three different sites at various decompositional stages using FTIR spectroscopy. *Geoderma* **1998**, *83*, 331–342. [[CrossRef](#)]



© 2018 by the authors. Licensee MDPI, Basel, Switzerland. This article is an open access article distributed under the terms and conditions of the Creative Commons Attribution (CC BY) license (<http://creativecommons.org/licenses/by/4.0/>).